An Intelligent Control of Solid oxide Fuel cell voltage

Kanhu Charan Bhuyan and Kamalakanta Mahapatra
Dept of ECE, National Institute of Technology-Rourkela, India-769008
Email: kanhu2006@gmail.com, kmaha2@rediffmail.com

Abstract— **This paper presents a comprehensive non-linear dynamic model of a solid oxide fuel cell (SOFC) that can be used for transient behaviors studies. The model based on electrochemical and thermal equations, accounts for temperature dynamics and output voltage losses. The relaxation time is strongly related to the transient temperature distribution of the solid oxide fuel cell structure. Therefore, it is in the order of some minutes depending on the design parameters and the operating conditions. The model contains the hydrogen, oxygen and water block separately. Other blocks are concentration, activation and ohmic losses block. The analytical details of how active and reactive power output of a stand-alone solid oxide fuel cell power plant (FCPP) is controlled. This analysis depends on an integrated dynamic model of the entire power plant including the reformer.**

Keywords— Fuel cell, FCPP, SOFC and Reformer.

I. INTRODUCTION

Many researchers reported on of Molten carbonate fuel cell. Looking back, in 2004, Francisco Jurada presented a model of 'Solid oxide fuel cell' without considering the temperature effect. The concept of molten carbonate fuel cell is exactly similar to solid oxide fuel cell. This comparison is given in [1] and [2]. The fuel input to the fuel cell is changing in steps in a paper in the literature[3]. Another very useful model is available in the literature which was suggested by Kourosh Sedghisigarchi, [3] and [4] .This paper considers all the subsystems of fuel cell, that includes hydrogen block, oxygen block, water block, activation and concentration block, and temperature block. In temperature block, the relaxation time is closely related to the transient temperature distribution of the solid oxide fuel cell structure. The internal cell resistances are strongly temperature dependent. Thus, the relaxation time depends on the thermal properties, size and configuration of the cell, and operating conditions. In [5] and [3], SOFC model is given without considering thermal unit. However, in this paper, these structures are modified by the modeling thermal unit. A first comprehensive nonlinear dynamic model of solid oxide fuel cell that can be used for dynamic and transient stability studies is developed by K. Sedghisigarchi, Ali Feliachi in 2004 [6]. The model based on electrochemical and thermal equations, accounts for temperature dynamics and voltage losses. The output voltage response of a stand-alone fuel-cell plant to a step change, a fuel flow step change, and fast load variations are simulated to illustrate the dynamic behavior of SOFC for fast and slow perturbations.

This paper presents a SOFC model and designs the control strategies for the AC voltage control and the active/reactive power control of the DC/AC inverter. Two separate controllers are designed for these purposes. The fuzzy logic control scheme is employed for the design of the two controllers.

II. PRINCIPLES OF FUEL CELL MODEL

The fuel cell (FC) is an electrochemical device that converts chemical energy of hydrogen gas (H_2) and oxygen gas (O_2) into electrical energy. The solid oxide fuel cell consists of two porous ceramic electrodes separated by a dense ceramic electrolyte. The cell produces electricity by the electrochemical reaction of fuel (hydrogen and / or carbon monoxide) and the oxidant (oxygen) across the solid electrolyte. Oxygen fed to the air electrode (cathode) accepts electrons from the external circuit to form oxygen ions. The ions are conducted through the solid electrolyte to the fuel electrode (anode). At the fuel electrode, the ions combine with hydrogen and/ or carbon monoxide in the fuel to form water and /or carbon monoxide. This reaction releases electrons. Electrons flow from the fuel electrode (anode) through the external circuit back to the air electrode (cathode).The overall reaction is exothermic; the cell produces heat in addition to electricity.

A typical fuel cell reaction is given below. The chemical reactions inside the cell that are directly involved in the production of electricity are given as

At Anode:

$$H_2 + O^{--} \rightarrow H_2O + 2e^-$$

$$CO + O^{--} \rightarrow CO_2 + 2e^{--}$$

At Cathode:

$$O_2 + 4e^{--} \rightarrow 2O_2^{\ -}$$

Overall:

$$H_2 + O_2 + CO \rightarrow H_2O + CO_2$$

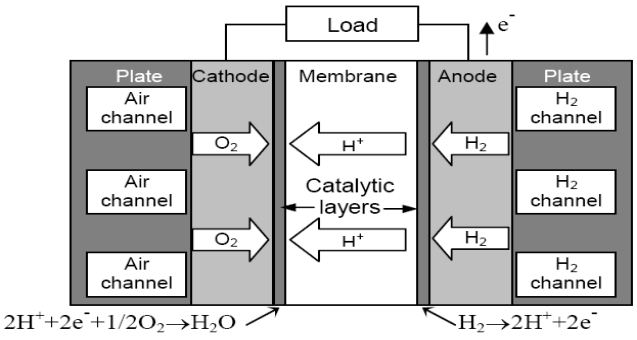

Fig. 1 Basic operation of Fuel Cell

978-1-4577-1510-5/11/$26.00 ©2011 IEEE

Model assumptions

The stack model is developed that uses following assumptions.

- The gases are ideal.
- The temperature is stable at all times.
- The Nernst equation can be applied.

The SOFC model consists of a) Electrochemical model-component material balance equations. b) Thermal model-Energy balance equations. c) Nernst voltage equation d) Reformer model. e) Power conditioning unit model. f) Active and reactive power control.

A. **Component material balance equation**

The change in concentration of each species that appears in the chemical reaction can be written in terms of input and output flow rates and exit molarities (x_i) due to the following chemical reaction

$$\frac{PV}{RT}_i \frac{d}{dt} x_i = N_i^{in} - N_i^0 + N_i^r \,. \quad (1)$$

where, V is compartment volume (m^3) , $N_{i,}^{in}$, N_i^0 are molar flow rates (mol/s) of i^{th} reactant at the cell input and output (exit), respectively. N_i^r is the reaction rate (mol/s) of the i^{th} reactant. T is the cell temperature in degree Kelvin, P is cell pressure (atom), R is the gas constant [(1 atom)/ (k mol degree Kelvin)].

Molar flow of any gas through the valve is proportional to its partial pressure inside the channel. The molar expression is given by

$$\frac{N_{H_2}}{x_{H_2}} = K_{H_2} \frac{N_{H_2O}}{x_{H_2O}} = K_{H_2O}$$

where, N_{H_2} is the hydrogen flow that reacts (k mol/s), K_i is the valve molar constant, x_i is the molar fraction of species.

Applying Laplace transformation to the above equation and isolating the hydrogen partial pressure, we obtain the following expression:

$$x_{H_2} = \frac{\frac{1}{K_{H_2}}}{1+\tau_{H_2 s}} \left(N^{in}{}_{H_2} - 2K_r I \right) \quad (2)$$

where , $\tau_{H2} = \frac{V}{K_{H2} RT}$,where, τ_{H2} expressed in seconds, is the time constant associated with hydrogen flow and is the function temperature, K_r is the constant dependent on Faraday's constant and number of electrons (N) in the reaction.

$$K_r = \frac{N}{4F}$$

where F is the Faraday's constant.

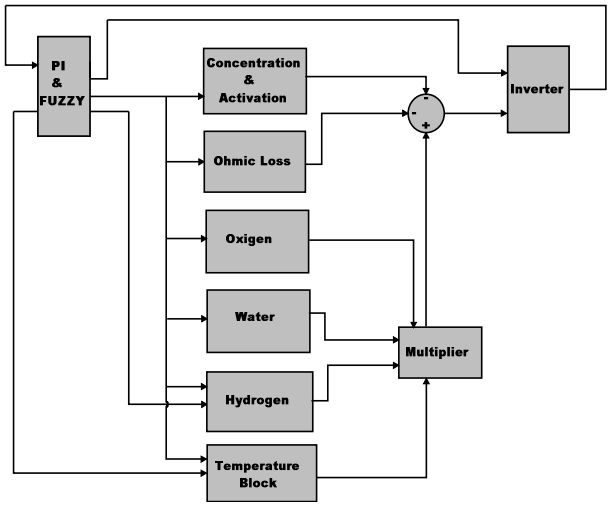

Fig. 2 SOFC Dynamic Model

B. **Thermal modeling**

The Nernst potential and loss mechanism are temperature sensitive; the temperature throughout the cell must be known to determine the cell's electrical performance accurately. Heat transfer occurs by the thermal conduction, convection and radiation. Conduction occurs in the solid cell materials and air free tube. Axial conduction in the solids is neglected due to long conduction path and reduces areas.

In addition to the various types of heat transfer and the sources, the thermal model also includes the variation of material properties with temperature. The fuel cell power output is closely related to the temperature of the unit cell. The heat storage in the thin fuel unit or oxidant gas layer is neglected. The thin fuel unit or oxidant gas layers are lumped to the cell unit and gas layers are assumed to have the same temperature as the unit cell.

E. Achenbach in [7] presents a relationship between two parameters S_0 and F_0 as given below

$$F_0 = 0.72 S_0^{-1.1} \quad (3)$$

where $F_0 = \frac{\lambda \Delta t}{\rho C_p h^2{}_{eff}}$ and $S_0 = \frac{U_j(1-\eta)}{\eta \lambda \Delta T} h_{eff}$

By simplifying the above eq. (3), we get

$$F_0^{0.909} = 0.72 S_0^{-1}$$

$$F_0^{0.909} = 0.72 \left(Y / \lambda \Delta T \right)^{-1} \quad (4)$$

where, $Y = \frac{U_j(1-\eta)}{\eta} h_{eff}$

U_j is the power density (electric output), η is the efficiency of the fuel cell, λ is the thermal conductivity, ΔT is change in temperature

From the above eq. (4) we get,

$$\Delta T = \frac{F_0^{0.909} Y}{0.72\lambda} \quad (5)$$

This is the increase in temperature from the initial condition after a relaxation time t .Assuming the relation between t, dt and temperature T . We can predict the temperature at on next simulation instant as

$$T_0 = T + \left(\frac{T_{in} + \Delta T - T}{t} \right) dt \quad (6)$$

C. Nernst voltage equation

Applying Nernst's equation and ohmic law (taking into account ohmic, concentration, and activation losses), the stack output voltage is represented by

$$V_{dc} = V_0 - rI - \eta_{act} - \eta_{con} \quad (7)$$

$$V_0 = N_0 \left(E^0 + \frac{RT^0}{2F} \ln \frac{x_{H_2} x_{O_2}^{\frac{1}{2}}}{x_{H_2O}} \right) \quad (8)$$

Where, (V_0) is open-circuit reversible potential (in volts), (E^0) is standard reversible cell potential, (x_i) is mole fraction of species, (r) is ohmic resistances(in ohms), (F) is Faraday's constant (coulomb per kilo mole), (T) is stack temperature in Kelvin, (N_0) is the number of cells in stack, η_{act} is activation losses in volts, η_{con} is concentration losses in volts, (I) is the stack current in amperes.

c.1) Activation loss

Activation polarization is present when the rate of an electrochemical reaction at an electrode surface is controlled by sluggish electrode kinetics. In the case of an electrochemical reaction with $\eta_{act} \geq$ 50-100mV, η_{act} is described by the general form of the Tafel equation:

$$\eta_{act} = \frac{RT}{\alpha nF} \log \left(\frac{i}{i_0} \right) \quad (9)$$

Where, (α) the electron is the transfer coefficient of the reaction at the electrode and (i_0) is the exchange current density. Voltage drop due to activation loss can be expressed by a semi –empirical equation, called the Tafel equation. It is given by

$$\eta_{act} = a + b \log i \quad (10)$$

Where $a = \left(\frac{-2.3RT}{\alpha nF} \right) \log i_0$ and $b = \frac{2.3RT}{\alpha nF}$ are called Tafel constant and Tafel slope respectively.

c.2) Concentration loss

The reactant is consumed at the electrode by electrochemical reaction; there is a loss of potential due to the inability of the surrounding material to maintain the initial concentration of the bulk fluid. At practical current densities, slow transport of reactants/ products to/from the electrochemical reaction site is a major contributor to concentration polarization:

$$\eta_{con} = \frac{RT}{n_a F} \ln \left(1 - \frac{i}{i_L} \right) \quad (11)$$

where (i), is the stack current, (i_L) is the limiting current and (n_a) is the number of electrons participating in the reaction.

c.3) Ohmic resistance loss

Ohmic losses occur because of resistance to the flow of ions in the electrolyte and resistance to flow of electrons through the electrode materials. This resistance is dependent on the cell temperature and is obtained by

$$r = \alpha \exp \left[\beta \left(\frac{1}{T_0} - \frac{1}{T} \right) \right] \quad (12)$$

where T is the stack temperature and α, β is the constant coefficients.

D. Reformer Model

In [8], the author introduced a simple model of a reformer that generates hydrogen through reforming methane. The model is a second order transfer function. The model can be written as follows:

$$\frac{q_{H_2}}{q_{methane}} = \frac{C_v}{\tau_1 \tau_2 s^2 + (\tau_1 + \tau_2) s + 1} \quad (13)$$

where, $q_{methane}$ is the methane flow rate [k mol/s], C_v is the conversion factor [k mol of hydrogen per kmol of methane], τ_1, τ_2 are the reformer time constants [s].

A proportional integral (PI) controller is used to control the flow rate of methane in the reformer [8]. Oxygen flow is determined using the hydrogen-oxygen flow ratio r_{H-O} .

E. Power conditioning Unit Model

The power conditioning unit is used to convert DC output voltage to AC. The power conditioning unit includes a DC/DC converter to raise DC output voltage, followed by a DC/AC inverter to convert the DC bus voltage to AC. In this paper, only a simple model of a DC/AC inverter is considered for the following reasons: the dynamic time constant of inverters is of the order of microseconds or milliseconds. The time constants for the reformer and stack are of the order of seconds.

A simple model of the inverter is given in [9], where output voltage and output power are controlled using the inverter modulation index and the phase angle δ of the AC voltage, V_{ac} . The output voltage and the output power as a function of the modulation index and the phase angle can be written as:

$$V_{ac} = m V_{cell} \angle \delta \quad (14)$$

$$P_{ac} = \frac{m V_{cell} V_s}{X} \sin(\delta) \quad (15)$$

$$Q = \frac{(mV_{cell})^2 - mV_{cell}V_s\cos(\delta)}{X} \quad (16)$$

where, V_{ac} is the AC output voltage of the inverter [V], m is the inverter modulation index, δ is the phase angle of the AC voltage mV_{cell} [rad], P_{ac} is the AC output power from the inverter [W], Q is the reactive output power from the inverter [VAR], V_s is the load terminal voltage [V], X is the reactance of the line connecting the fuel cell to the infinite bus [Ω].The voltage at the load terminals is considered constant. PI controllers are used to control the modulation index.

F. Active and Reactive Power Control

In traditional synchronous generators, the amount of steam input to the turbine controls the power angle, which controls the active power output from the generator. In synchronous machines, the power angle is not measured, but the adjustment of the power angle occurs following changes in steam input and rotor speed. In the FCPP, there is no speed control but the similar relationship between output voltage phase angle and the flow of hydrogen can be adopted as follows. Given that the load voltage $(Vs\angle 0)$ is constant and the AC source voltage out of the inverter V_{ac} is given in (14), the angle δ controls the power flow from the fuel cell to the load, as in (15). The phase angle δ can be controlled using the input flow of hydrogen. The expression for δ , therefore, provides the relationship between the power output as a regulated quantity, and the amount of flow of fuel input. This relationship is described by the following equations:

Assuming a lossless inverter, we get

$$P_{ac} = P_{dc} = V_{cell}I \quad (17)$$

According to the electrochemical relationships, a relationship between the stack current and the molar flow of hydrogen can be written as

$$q_{H_2} = \frac{N_0 I}{2FU} \quad (18)$$

From equations (15), (17), and (18)

$$\sin\delta = \frac{2FUX}{mV_s N_0} q_{H_2} \quad (19)$$

Assuming a small phase angle $\sin\delta \cong \delta$; (19) can be written as

$$\delta = \frac{2FUX}{mV_s N_0} q_{H_2} \quad (20)$$

Equation (20) describes the relationship between output voltage phage angle δ and hydrogen flow q_{H_2}. Equations (15) and (20) indicate that the active power a function of the voltage phase angle δ can be controlled by controlling the amount of hydrogen flow.

III.TS Fuzzy Controller

The proportional plus integral (PI) controller requires precise linear mathematical models, which are difficult to obtain and may not give satisfactory performance under the transient conditions. The advantage of fuzzy logic controller is that it does not require a mathematical model of the system. Here in the paper, TS fuzzy controller is incorporated because of its simple structure. The linguistic rule consequent is made variable by means of its parameters. As the rule consequent is variable, the TS fuzzy control scheme can produce an infinite number of gain variation characteristics. In essence, the TS fuzzy controller is capable of offering more and better solutions to a wide variety of non-linear control problems.

The deviations in the power error (error between reference and actual powers) are fuzzified using two input fuzzy sets P (positive) and N (negative). The membership function used for the positive set is

$$\mu_P(x_i) = \begin{cases} 0 & x_i < -L \\ \dfrac{x_i + L}{2L} & -L \le x_i \le L \\ 1 & x_i > L \end{cases} \quad (21)$$

Where, $x_i(k)$ denotes the input to the fuzzy controller at the k^{th} sampling instant given by

$$x_1(k) = e(k) = P_{acref} - P_{ac} \quad (22)$$

and

$$x_2(k) = \sum e(k) \quad (23)$$

For the negative set is

$$\mu_N(x_i) = \begin{cases} 1 & x_i < -L \\ \dfrac{-x_i + L}{2L} & -L \le x_i \le L \\ 0 & x_i > L \end{cases} \quad (24)$$

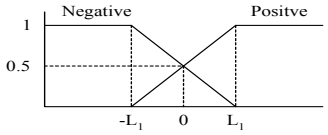

(a)

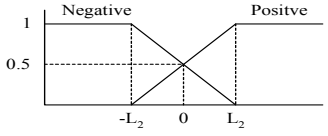

(b)

Fig. (3) Membership function for (a) x_1 and (b) x_2

The membership functions for x_1 and x_2 are shown in figures (3) (a) and (b) respectively. The values of L_1 and L_2 are chosen on the basis of maximum value of error e and its integration. The TS fuzzy controller uses the four simplified rules as

R1: If $x_{1(k)}$ is P and $x_2(k)$ is P then $u_1(k) = a_1.x_1(k) + a_2.x_2(k)$

R2: If $x_1(k)$ is P and $x_2(k)$ is N then $u_2(k) = K_2\ u_1(k)$

R3: If $x_1(k)$ is N and $x_2(k)$ is P then $u_3(k) = K_3\ u_1(k)$

R4: If $x_1(k)$ is N and $x_2(k)$ is N then $u_4(k) = K_4\ u_1(k)$

In the above rules, u_1, u_2, u_3, u_4 represents the consequent of the TS fuzzy controller. Using Zadeh's rule for AND operation and the general defuzzifier, the output of the TS fuzzy controller is

$$u(k) = \frac{\sum_{j=1}^{4} (\mu_j)^{\gamma}\ u_j(k)}{\sum_{j=1}^{4} (\mu_j)^{\gamma}} \qquad (25)$$

However for γ=1, we get the centroid defuzzifier with $u(k)$ given by

$$u(k) = a\,x_1(k) + b\,x_2(k)$$

where $a = a_1 K, \quad b = a_2 K$ and

$$K = (\mu_1 + K_2\mu_2 + K_3\mu_3 + K_4\mu_4)/(\mu_1 + \mu_2 + \mu_3 + \mu_4)$$

As K is operating condition dependent, the effective value of control gain varies widely during the control process. The values of a_1, a_2; K_2; K_3; K_4 are given in APPENDIX-B.
In the similar fashion TS fuzzy is incorporated to control reactive power. This concept is given in [10].

IV. RESULTS AND ANALYSIS

Fuel cell is designed for 320 V D.C. output voltage. Fig. 4 shows the output voltage of fuel cell. Temperature of fuel cell is dependent on active power requirement. Consider that active power is increased from 0.3 p.u. to 0.6 p.u at 1000 sec. and then decreased to 0.3 p.u at 2000 sec.. Maintaining reactive power constant; the temperature of fuel cell is changed accordingly as shown in Fig. 5.

Fig. 6 and 7 shows the active and reactive powers which are dependent on each other. The active power requirement is changed from 0.2 p.u to 0.6 p.u at 200 sec. and again it is changed to 0.4 p.u at 300 sec. From Fig. 6, it is seen that fuel cell is capable of providing the active power requirement. As active power demand is changed, the reactive power will also change Fig. 7 shows the capability of fuel cell to meet the reactive power demand. In order to make reactive power requirement independent of active power, a decoupled control theory is used. Consider that the active power is kept constant at 0.5 p.u. as shown in Fig. 8 and reactive power demand is increased from 0.2 p.u to 0.6 p.u at 200 sec and then decreased to 0.4 p.u at 300 sec. Fig. 9 shows the capability of fuel cell to meet reactive power requirement which is controlled independently by applying decoupled control.

Let initially rms value of active power is 30 kW and if the demand is that this rms value changes sinusoidally i.e., Pacref changes at 200 secs. Fig. 10 shows that the fuel cell with PI controller is tracking the required reference power (Pacref), but it does not track the reference power perfectly.

To overcome this problem, TS fuzzy controller is incorporated (discussed earlier). Fig. 11 shows the tracking performance of fuel cell with TS fuzzy controller. From Fig. 11, it is seen that TS fuzzy controller is tracking the reference power perfectly. Now consider that reference active power changes (Pacref) shown in Fig. 10 and 11 shows the performance of fuel cell with PI controller and Fig.11 shows the performance with TS fuzzy controller. From these figures, it is seen that TS fuzzy controller can meet the power demand perfectly as compared to PI controller. In the similar fashion the reactive power demand is changed and performance of fuel cell with PI controller and TS fuzzy controller is observed in figures 12 and 13. From these figures, it is seen that TS fuzzy controller can track the required reactive power demand perfectly as compared to PI controller.

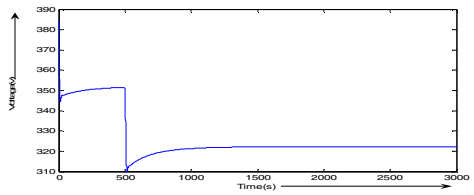

Fig. 4 Fuel cell output DC Voltage

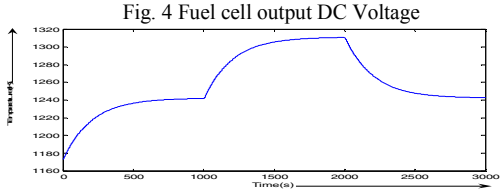

Fig.5 Temperature of fuel cell

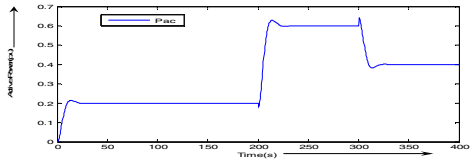

Fig. 6 Active power

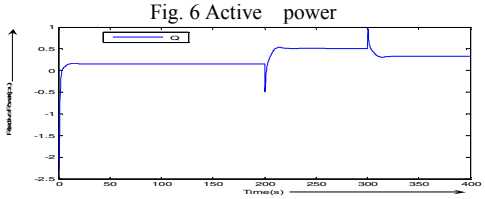

Fig.7 Reactive power

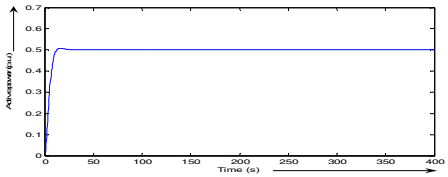

Fig. 8 Active power (decoupled control)

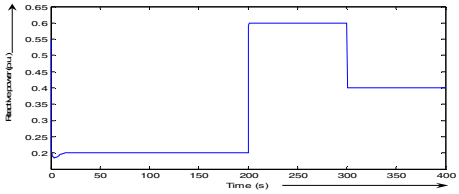

Fig. 9 Reactive power (decoupled control)

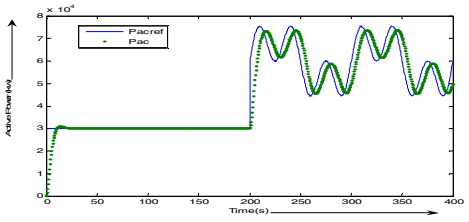

Fig. 10 Active Power with PI controller

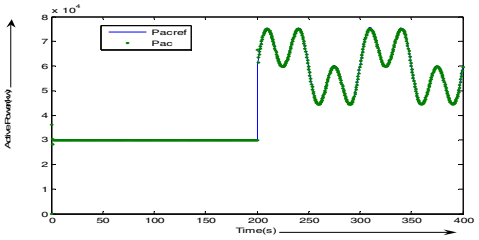

Fig. 11 Active powers with Fuzzy controller

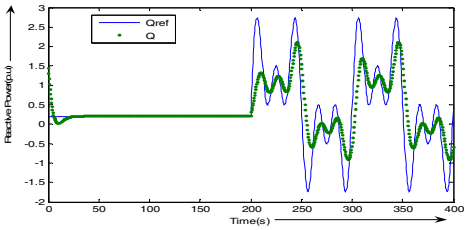

Fig.12 Reactive powers with PI controller

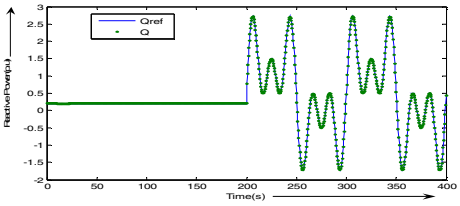

Fig. 13 Reactive power with fuzzy controller

V. CONCLUSIONS

The proposed SOFC dynamic model is developed along with the subsystems of concentration block, activation block, water, oxygen and hydrogen block. Thermal block is also incorporated in the SOFC dynamic model. The integrated model includes fuel cell and power conditioning unit. The mathematical equations facilitate modeling DC to AC converter. The proposed model is tested with its active and reactive power outputs being compared with the required load demand. The dynamic behavior of SOFC model is analyzed by using PI and TS fuzzy controller separately. Here TS fuzzy logic controller is chosen because of its simple structure. It is observed that the dynamic performance of fuel cell with TS fuzzy controller is better in terms of tracking power demand as compared to the PI controller.

REFERENCES

[1] M.D. Lukas, K.Y Lee. And H.Ghezel-Ayagh, "Development of a stack Simulation model for Control Study on direct reforming molten carbonate Fuel Cell Power Plant," *IEEE Trans. Energy Conversion*, Vol.14, pp.1651-1657, Dec.1999.

[2] Wolfgang Friede, Stephane Rael, and Bernard Davat, "Mathematical Model and characterization of the Transient Behaviour of a PEM Fuel Cell,'' *IEEE Trans. on Power Electronics*, Vol.19. No5, September 2004

[3] K.Sedghisigarchi, and Ali Feliachi, "Dynamic and Transient analysis of Power distribution systems with Fuel Cells- Part II: Control and stability Enhancement.

[4] J.Padulles, G.W. Ault, and J. R. McDonald, "An integrated SOFC plant dynamicmodel for power system simulation," *J. Power Sources*, pp.399-408, Mar.1993.

[5] M.Y. El-Sharkh, A. Rahman, M.S. Alam, A.A. Sakla, "Analysis of Active and Reactive Power Control of a Stand-Alone PEM Fuel Cell Power Plant," *IEEE Trans. on Power Systems*, Vol.19, No. 4, November 2004

[6] K. Sedghisigarchi, Ali Feliachi, "Dynamic and Transient Analysis of power distribution systems with fuel cell,''- Part I Fuel-cell Dynamic Model *IEEE Transactions on Energy Conversion*, Vol, 19, No.2, June 2004.

[7] E. Achenbach, "Three dimensional and time dependent simulation of planar SOFC stack," *J.power Sources*, Vol.49, 1994.

[8] M.Y. El-Sharkh, A. Rah man, M. S. Alam, " Neural networks-based control of active and reactive power of a stand-alone PEM fuel cell power plant,'' *J.Power Sources* 135(2004) 88-94.

[9] Y.H. Kim, and S.S. Kim, "An Electrical Modeling and Fuzzy Logic Control of a Fuel Cell generation System," *IEEE Trans. On Energy Conversion*, Vol.14, No.2, June 1999.

[10] D.J Hal and R.G Colclaser, "Transient Modeling and Simulation of Tabular Solid Oxide Fuel Cell," *IEEE Trans. Energy Conversion*, Vol.14, pp.749-753, Sept.1999.

APPENDIX-A: Fuel Cell Operating Data

Temperature(T)	$900\ ^0K$
No load voltage (E_0)	1V
Number of cells (N_0)	384
Utilization factor (U)	0.8
Reformer time constant (τ_1)	2 s
Reformer time constant (τ_2)	2 s
Conversion factor (C_v)	2
Line reactance (X)	$0.05\ \Omega$
PI gain constants $(K_{p,}K_I)$	0.1
Base Voltage (V_r)	400V
Methane reference signal $(Q_{methref})$	0.000015 kmol/s
Hydrogen-Oxygen flow ratio (r_{H-O})	2
Base MVA	100KVA

APPENDIX-B

For Active power control: a_1=10, a_2; =100, K_2;= K_3; =K_4=1
For Reactive power control: a_1=0.1, a_2; =10, K_2;= K_3; =K_4=0